Superalloys 2008
Roger C. Reed, Kenneth A. Green, Pierre Caron, Timothy P. Gabb, Michael G. Fahrmann, Eric S. Huron and Shiela A. Woodard
TMS (The Minerals, Metals & Materials Society), 2008

INVESTIGATION OF THE PARTITION COEFFICIENTS IN THE NI-FE-NB ALLOYS: A THERMODYNAMIC AND EXPERIMENTAL APPROACH

Jairo Valdes*, DongEung Kim+, Shun-Li Shang+, Xingbo Liu**, Paul King++, Zi-Kui Liu+
*West Virginia University WV, USA, Universidad del Valle, Cali-Colombia
+ Department of Material Science and Engineering, The Pennsylvania State University, University Park, PA 16802, USA
** Department of Mechanical and Aerospace Engineering, West Virginia University, Morgantown, WV 26506, USA
++ DOE-NTEL, Albany, OR 97321-2198, USA

Keywords: partition coefficient, thermodynamic, Ni-Fe-Nb

Abstract

The Nb containing Ni-based superalloys used for the production of large castings are highly sensible to the formation of macrosegregation defects like freckles and white spots. Production cost can be reduced by better prediction of the freckle formation. The most accepted freckling criterion is the one based on the Rayleigh number, which requires accurate determination of the partition coefficients for the solute elements. In this work, the partition coefficients of Nb and Fe on the ternary system Ni-Fe-Nb were studied by experimental measurements and by thermodynamic calculations. Modified DTA experiments were performed for model alloys, and a thermodynamic database for the Ni-Fe-Nb ternary system was developed. Most of the calculated partition coefficients using the developed model agree well with the experimental data. One exception to this, as will be discussed later, is the partitioning coefficient of Fe for the alloy containing 36 wt. %Fe.

Introduction

Efficient and environmentally friendly energy production can be obtained by increasing the firing temperature and the size of the land based gas turbines. It is reported that every 50°F increase of the firing temperature results in a 1% improvement of combined-cycle efficiency[1]. The large rotor discs required need to be made of Nb containing Ni based superalloys to avoid over aging[2] and withstand the higher operation temperatures. However, Nb containing alloys tend to present macrosegregation defects like freckles, caused by downward flow of segregated heavier interdendritic liquid, in the mushy zone of the u-shaped metal pool characteristic of the Vacuum Arc Remelting (VAR) ingots[3]. In order to avoid freckles special melting techniques at increased cost have been developed to produce the large VAR ingots, which include multiple stages of remelting combined with liquid metal refining steps and rigorous computer control of the process[4, 5]. Production cost could be reduced by a better prediction of freckle formation using a criterion that accurately describes the physical phenomenon. The criterion most widely used is based on the Rayleigh number concept and is strongly influenced by the density change of the interdendritic liquid, requiring accurate determination of the partition coefficients of solute elements and their variation with the evolution of the solidification. As Ni based superalloys are usually multicomponent, computational modeling can provide tractable approaches to gain insights into how the partition coefficients change as a function of temperature, composition and processing conditions.

The main objective of this work is to study the partition coefficients of Nb and Fe in the model Ni-base alloys and compare the measurements with the theoretical predictions. The Ni-based alloy samples were prepared by mixing and melting the raw elements using a tri-arc bottom furnace. The partition coefficients were measured on samples by modified DTA experiments (MDTA) on which the samples were quenched while solidifying. Two databases were used to predict partition coefficients: Ni-Fe-Nb system obtained by this work and the TTNi6 Ni-database[6]. The thermodynamic database of the Ni-Fe-Nb ternary system has not been reported in the literature, and was developed in the present work. The calculations were performed using two different methods: (i) the equilibrium solidification model[7] and (ii) the Scheil model[8].

Experimental Approach

The samples of the Ni-Nb-Fe system were prepared with two levels of variation on the contents of solutes. In the case of Nb the amounts were 3 and 5 (wt. %), while for Fe the contents were selected to be 5 and 36 (wt. %). A high purity Argon atmosphere was used and multiple steps of melting were performed to attain good composition homogeneity. Regular DTA experiments were carried out to define the temperature range of the mushy zone for the isothermal and subsequent quench steps during the quenching modified DTA experiments (MDTA). To perform the MDTA experiments, the thermocouple assembly of the standard differential calorimeter was modified to permit locating a quenching oil bath in the bottom of the alumina tube furnace as shown in the Fig. 1. On the top of the alumina rod which contains the sample and reference thermocouples, a solidified sample with the typical semispherical shape can be observed. In all experiments, a 10 cm^3/min flow of high purity Argon was used. All samples were heated up to temperatures above the liquidus transformation at a 10 C/min rate and slowly cooled to the mushy zone temperature region (5 C/min). A short duration isothermal step preceded the quenching step which was executed by tapping off the sample from the rod to the quenching oil. In the preliminary regular DTA experiments it was observed that the solidus temperature was more sensitive to variations in the

thermal conditions that affect the experiments (wider variation range), than the liquidus, as expected by theoretical result shown in Fig. 2. It shows that the diffusion rates of alloying elements in the solid and liquid phases affect significantly the predicted solidus temperature.

Measurement of the Partition Coefficients

The SEM/EDS analysis of the quenched samples suggested that the 5 C°/min cooling rate before quenching was slow enough to maintain local equilibrium in the primary solid–liquid interface with no solute entrapment and negligible back diffusion, indicating the Scheil model was still applicable[9]. For quenched high Nb content samples, the chemical composition was measured by SEM/EDS micro probe analysis along arbitrary oriented scan lines over primary gamma dendrites. Point measurements over interdendritic areas were discarded for the segregation profile fitting as suggested by Gungor[10]. The data was ranked and assigned an apparent solid fraction according to the segregation tendency following the methodology proposed by Flemings et al[11]. The solid volume fraction at the temperature of quenching was determined by areal measurement using Hillard's quantitative metallography analysis[12].

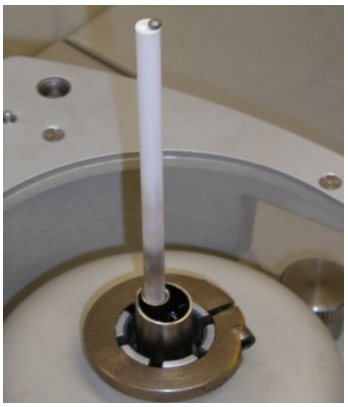

Fig.1. Experimental MDTA setup used for the quenching experiments.

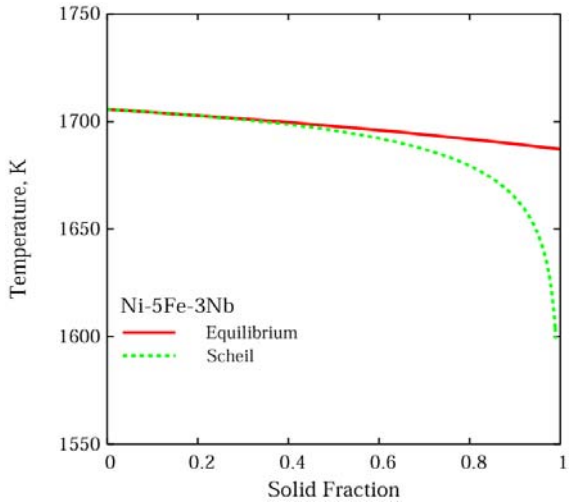

Fig. 3. Calculated transition temperature as a function of solid fraction of Ni-5Fe-3Nb by two different methods.

Fig. 3 shows a backscattered electrons SEM image on which can be identified the dendritic structure along with the interdendritic eutectic, composed of Nb_7Ni_6 (μ) lamellar phase and eutectic gamma.

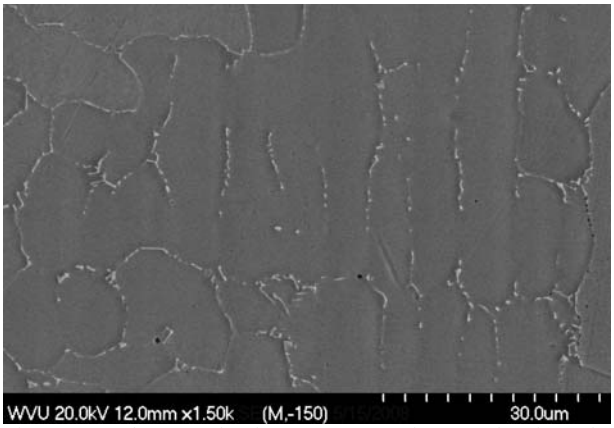

Fig. 3. Backscattered electrons SEM image showing the microstructure found on the quenched Ni-5Fe-3Nb model alloy.

A higher magnification backscattered electrons image is presented in Fig. 4, where a composition scan was taken covering secondary arm dendrites and the interdendritic eutectic between them.

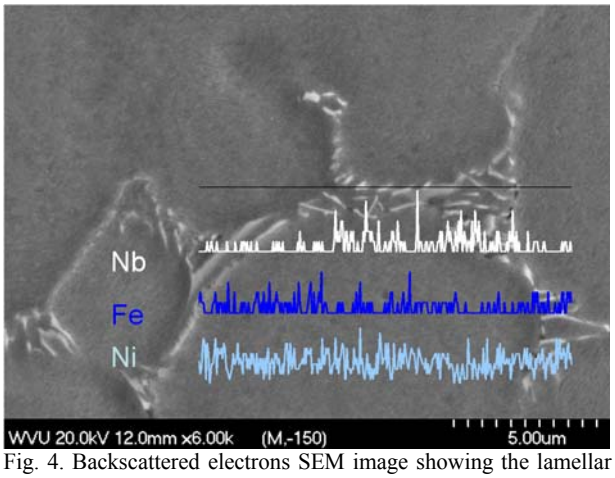

Fig. 4. Backscattered electrons SEM image showing the lamellar eutectic (μ phase + gamma) between secondary arm dendrites.

The solute profiles were then fitted to the Scheil equation and the partition coefficients were determined by minimizing the squared error. Fig. 5 gives an example showing the fitting error of segregation profile to the Scheil model for Ni-5Fe-5Nb sample alloy. The obtained partition coefficients of Nb and Fe by Scheil fitting method are presented in table 1. In general, the cumulative curves of solid fraction vs. solute composition fit well with the Scheil model description in accordance to the results obtained by Lacaze et al. for the quenched samples with 0.7 solid volume fraction[13].

Determination of the initial partition coefficients was performed for the low Nb content samples using area scanning measurements representing the average chemical composition of the primary dendrites and the overall composition of the eutectic constituent.

The obtained results are included in Table 1. For this experimental methodology, it was assumed that the overall composition measured on the eutectic constituent area represent the liquid composition at the temperature of quenching.

Ni-Fe-Nb system

Binary Systems

Recently, the Fe-Ni system was remodeled[14] to consider the ordering in the γ-$FeNi_3$ phase. The Fe-Nb and Ni-Nb binary systems were also remodeled by Toffolon[15] and Chen[16], respectively. These three binary systems are in better agreements with the experimental data than the TTNi6 Ni-database[6], especially Laves (Fe_2Nb) phase in the Fe-Nb system and μ (Nb_7Ni_6) phase in the Ni-Nb system.

The μ phase is one of the stable phases in the Fe-Nb and Nb-Ni binary systems, but different sublattice models were introduced, i.e., $(Fe,Nb)_1(Nb)_4(Fe,Nb)_2(Fe)_6$ used in the Fe-Nb system[15], whereas $(Nb,Ni)_1(Nb)_4$ $(Nb,Ni)_2(Nb,Ni)_6$ employed in the Nb-Ni system[16]. The sublattice model of the same phase in the binary systems needs to be consistent in order to model the ternary system.

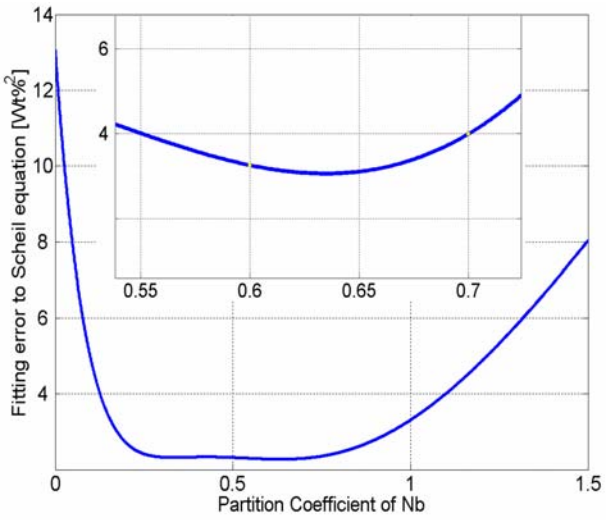

Fig. 5. Fitting error of segregation profile to the Scheil model in Ni-5Fe-5Nb alloy

In the present work, the sublattice model of μ phase in the Fe-Nb system was changed to allow the element Nb to enter into the forth sublattice. A value of 5000 J/mol-atom was assigned for the end members of pure element sides according to the work of Coelho et al[17]. Other parameters to describe the μ phase were obtained through the PARROT module in Thermo-Calc[18]. The Fig. 6 shows that the presently modeled μ phase (Fe_7Nb_6) in the Fe-Nb system agrees well with the previous work by Toffolon[15].

Development of the Ternary System

Based on the three binary systems, the Ni-Fe-Nb ternary system has been modeled herein. The compositions of ternary alloys measured at 1473K by Takeyama et al.[19] were employed to model the ternary interaction parameters of the liquid phase. In the present work, ternary intermetallic compounds were ignored, though one compound with hexagonal structure was reported at composition around Ni-22Nb-20Fe (at.%)[19], but the detailed information is still not available for this compound such as the melting point and enthalpy of formation, etc.

Table I. Summary of the measurements of the partition coefficients of Nb and Fe

MDTA Experiment sample	Assumptions	Mean partition coefficients	
		K_{Nb}	K_{Fe}
Ni-5Fe-3Nb	Overall composition. of eutectic constituent equal to C_L	0.52	1.03
Ni-36Fe-3Nb		0.30	1.59
Ni-5Fe-5Nb	Scheil fitting	0.63	1.05
Ni-36Fe-5Nb		0.29	1.05

Fig. 7(a) and Fig. 7(b) are the calculated isothermal sections at 1473K of the Ni-Fe-Nb system using the presently modeled parameters and the TTNi6 Ni-database, respectively, compared with the experimental results[19].

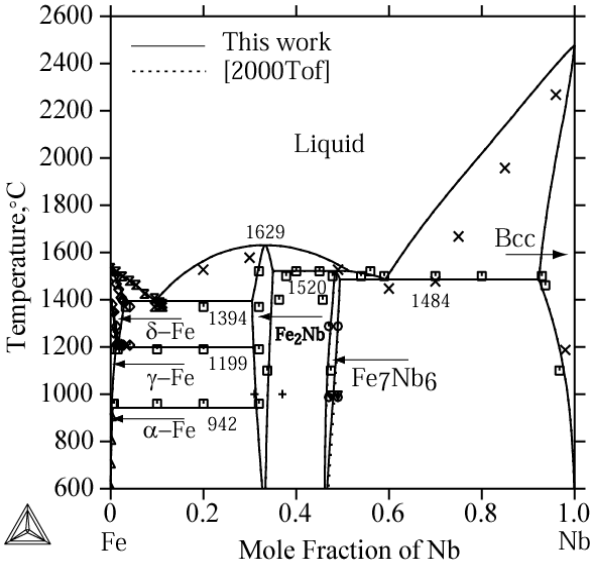

Fig. 6. Phase diagrams of the Fe-Nb system in this work (solid line) and by Toffolon[15] (dotted line). All symbols are the experimental data used in Toffolon's work[15].

The open circles and closed circles indicate the bulk alloy composition and phase boundary data, respectively[19]. The current ternary description shows better agreement with the experimental data than the TTNi6 Ni-database. All open circles should be in the two-phase regions but some of them in the Fig. 7(b) are in the three-phase regions. The phase boundaries of the Laves phase and the Ni_3Nb phase in the current work are also described well in comparison with those in the TTNi6 Ni-database.

Prediction of Partition Coefficient for the Ni-Fe-Nb Alloys

The partition coefficients of Fe and Nb in the Ni-Fe-Nb alloys were calculated based on the current model and the TTNi6 Ni-database. Fig. 8 illustrates the calculated partition coefficients of

Nb and Fe as a function of solid fraction in the Ni-5Fe-3Nb and Ni-36Fe-5Nb (wt. %) alloys by equilibrium calculations. Experimental results for the initial partition coefficients are included. In Fig. 9, the results using the Scheil model are presented including the experimental results obtained by Scheil equation fitting. Fig. 8 shows that the partition coefficient of Fe increases as increasing the content of Fe in the alloy while, in case of Nb, the partition coefficient decreases for both the current model and the TTNi6 Ni-database. The same tendencies were observed for equilibrium and Scheil calculations (cf. Fig. 9).

Comparing with Theoretical Values

The experimental analysis of MDTA samples of the Ni-Fe-Nb system by the methodology of fitting to Scheil equation showed that the partition coefficient of Nb decreased with the increase of Fe content (higher segregation tendency), in agreement with the thermodynamic modeling of the ternary Ni-Fe-Nb system performed using both the database developed in the present work and the TTNi6 Ni-database[6]. This result is in accordance to the experimentally determined trend reported by Yang et al.[20] for commercial superalloys with different amounts of Fe, and with the redistribution modeling results reported by DuPont et al.[21]

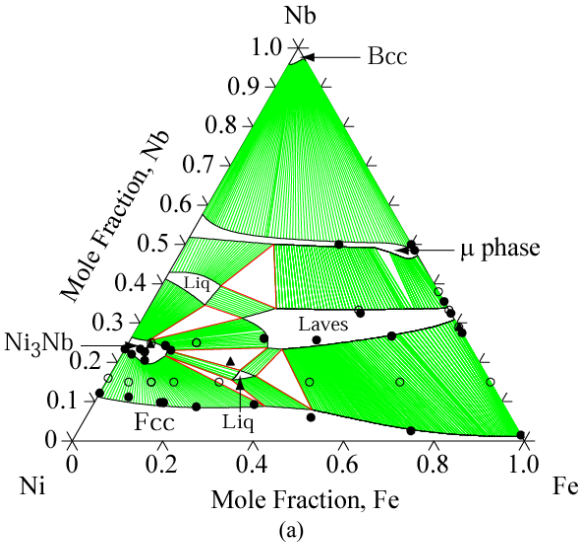

The cumulative curves of solute elements Nb and Fe did not show the negative curvature observed in previous experimental studies that was attributed to limited diffusion in the liquid phase. The rapid cooling in the quenching step limited the diffusion and could not permit the intermixing of the buildup of solute elements. This result supports the explanation that associates the negative curvature with noise of the X-ray measurements[22].

Fig. 8 shows that most of measurements have good agreement with the equilibrium predicted values; however there is a relatively large difference for the partition coefficient of Fe of Ni-36Fe-5Nb. The same trend was observed in Fig. 9 when the Scheil model was used. The difference, which remains to be resolved, could be associated to the fact that the solidification on the experiments occurred in global conditions that depart from equilibrium, but it seemed to be more likely related to difficulties in the measurement, because the predicted values from both the current model and the TTNi6 Ni-database are similar.

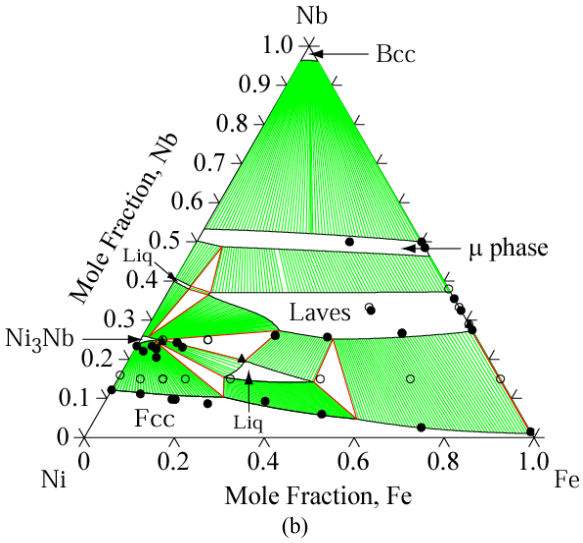

Fig. 7. Calculated isothermal section of the Fe-Ni-Nb system at 1473K by (a) the present model and (b) the TTNI6 Ni-database [6], together with the measured two phase region (open cycles), the phase boundary data (closed cycles)[19] and the liquid phase (triangle).

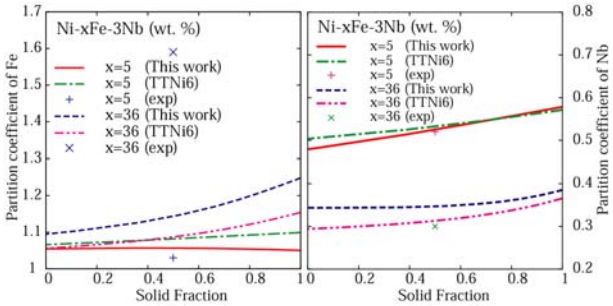

Fig.8. Calculated partition coefficients of Fe and Nb as a function of solid fraction in the Ni-xFe-3Nb (wt. %) by equilibrium calculations using the current model and the TTNI6 Ni-database.

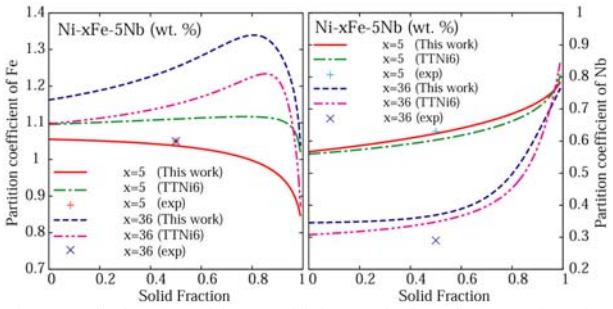

Fig. 9. Calculated partition coefficients of Nb and Fe as a function of solid fraction in the Ni-xFe-5Nb (wt. %) by the Scheil model using the current model and the TTNi6 Ni-database.

Summary

Experimental measurements of the partition coefficients of Nb and Fe were obtained for different compositions of the Ni-Fe-Nb ternary system. Computational thermodynamic modeling of the

Ni-Fe-Nb ternary system is performed based on three binary systems and the available experimental data. The sublattice model for the μ phase in the Fe-Nb binary system was also updated to keep consistency with the Nb-Ni binary system. The partition coefficients of the current model and the TTNI6 Ni-database are calculated and they agree with experimental data but it is shown that the measured partition coefficients of Fe for the alloy containing Fe of 36 wt. % have relatively large differences with the calculated results. The discrepancies remain to be resolved.

REFERENCES

1. P. W. Schilke and R. C. Schwant. Alloy 706 Use, Process Optimization, and Future Directions for GE Gas Turbine Rotor Materials, *Superalloys 718, 625, 706 and Various Derivatives. Ed: E.A. Loria. Warrendale, Journal of the Minerals Metals & Materials Society*, (2001), 25-34.

2. R. C. Schwant, et al. Large 718 forgings for land based turbines, *Superalloys 718, 625, 706 and Various Derivatives, Proceedings of the International Symposium on Superalloys 718, 625, 706 and Various Derivatives, 4th, Pittsburgh, June 15-18, 1997*, (1997), 141-152.

3. J. A. Van Den Avyle, J. A. Brooks, and A. C. Powell. Reducing defects in remelting processes for high-performance alloys, *Journal of the Minerals Metals & Materials Society*, 50 (3) (1998), 22-+.

4. C. Malare and J. Radavich. *Superalloys 718, 625, 706 and Various Derivatives, E.A. Loria, Ed., The Minerals, Metals and Materials Society, Pittsburg, PA*, (2005), 25-33.

5. A. D. Patel, R. S. Minisandram, and D. G. Evans. Modeling of vacuum arc remelting of Alloy 718 ingots, *Superalloys 2004, Proceedings of the International Symposium on Superalloys, 10th, Champion, PA, United States, Sept. 19-23, 2004*, (2004), 917-924.

6. N. Saunders and A. P. Miodownik. TTNi6, TT Ni-based Superalloys Database (Version 6.0, Jul. 2003), http://www.thermocalc.com/Products/Databases/TTNi6.htm, (1998).

7. G. H. Gulliver. The quantitative effect of rapid cooling upon the constitution of binary alloys, *Journal of the Institute of Metals*, 9 (1913), 120-154.

8. E. Scheil. *Zeitschrift fuer Metallkunde*, 34 (1942), 70-72.

9. J. A. Sarreal and G. J. Abbaschian. The Effect of Solidification Rate on Microsegregation, *Metallurgical Transactions a-Physical Metallurgy and Materials Science*, 17 (11) (1986), 2063-2073.

10. M. N. Gungor. A Statistically Significant Experimental-Technique for Investigating Microsegregation in Cast Alloys, *Metallurgical Transactions a-Physical Metallurgy and Materials Science*, 20 (11) (1989), 2529-2533.

11. M. C. Flemings, et al. Microsegregation in Iron-base Alloys, *Journal of the Iron and Steel Institute*, 208 (1970), 371-&.

12. J. E. Hillard. Volume-fraction analysis by quantitative metallography, *General Electric report*, (1961).

13. J. Lacaze and G. R. J. Lesoult. Experimental Investigation of the Development of Microsegregation during Solidification of an Al-Cu-Mg-Si Aluminum-Alloy, *Materials Science and Engineering a-Structural Materials Properties Microstructure and Processing*, 173 (1-2) (1993), 119-122.

14. T. Honda. Unpublished work, *Pennsylvania State University*, (2007).

15. C. Toffolon and C. Servant. Thermodynamic assessment of the Fe-Nb system, *Calphad-Computer Coupling of Phase Diagrams and Thermochemistry*, 24 (2) (2000), 97-112.

16. H. L. Chen and Y. Du. Refinement of the thermodynamic modeling of the Nb-Ni system, *Calphad-Computer Coupling of Phase Diagrams and Thermochemistry*, 30 (3) (2006), 308-315.

17. G. C. Coelho, et al. Thermodynamic optimization of the Nb-Fe and Ta-Fe binary systems, *Processing and Applications of High Purity Refractory Metals and Alloys; Pittsburgh, Pennsylvania; United States; 17-21 Oct. 1993*, (1994), 51-70.

18. J. O. Andersson, et al. THERMO-CALC & DICTRA, computational tools for materials science, *Calphad-Computer Coupling of Phase Diagrams and Thermochemistry*, 26 (2) (2002), 273-312.

19. M. Takeyama, et al. Phase Equilibria Among γ, Ni3Nb-δ and Fe2Nb-ε Phases in Ni-Nb-Fe and Ni-Nb-Fe-Cr Systems at Elevated Temperatures, *Superalloys 718, 625, 706 and Various Derivatives, E.A. Loria, Ed., The Minerals, Metals and Materials Society*, (2001), 333-344.

20. W. Yang, et al. Segregation and solid evolution during the solidification of niobium-containing superalloys, *Superalloys 2000, Proceedings of the International Symposium on Superalloys, 9th, Seven Springs, PA, United States, Sept. 17-21*, (2000), 75-84.

21. J. N. Dupont, C. V. Robino, and A. R. Marder. Modeling solute redistribution and microstructural development in fusion welds of Nb-bearing superalloys, *Acta Materialia*, 46 (13) (1998), 4781-4790.

22. J. Lacaze and G. Lesoult. Modeling the Development of Microsegregation during Solidification of an Al-Cu-Mg-Si Alloy, *Isij International*, 35 (6) (1995), 658-664.